A high resolution threshold electron spectrometer for use in photoionisation studies

J. Phys. E: Sci. Instrum. **20** (1987). Printed in the UK

A high resolution threshold electron spectrometer for use in photoionisation studies

G C King, M Zubek†, P M Rutter and F H Read
Department of Physics, Schuster Laboratory, Manchester University, Manchester M13 9PL, UK

Received 22 May 1986, in final form 31 July 1986

Abstract. An electron spectrometer is described for use in threshold photoionisation studies. The spectrometer incorporates a penetrating field extractor stage, a 127° cylindrical deflection analyser and an electrostatic lens system to match the two together. The high collection efficiency, resolution, transmission and sensitivity of the spectrometer are demonstrated with threshold photoionisation measurements in argon and helium. The spectrometer is also able to handle non-threshold photoelectrons. The high performance and ease of operation of the spectrometer suggest that it could be used as a general diagnostic tool on synchrotron VUV and soft x-ray beam lines.

1. Introduction

Threshold photoelectron spectroscopy has been shown to be a powerful technique in the study of photoionisation of atoms and molecules (see, for example, Peatman *et al* 1969, 1978, Delwiche *et al* 1981). The technique allows the direct and accurate determination of ion excitation energies and the measurement of photoionisation cross sections close to their thresholds rather than far above the thresholds as in conventional photoelectron spectroscopy, which it therefore complements. Important advantages of threshold photoelectron spectroscopy over conventional photoelectron spectroscopy at fixed wavelength are that very high transmission can be achieved for electrons of near-zero kinetic energy without loss of energy resolution and that Doppler broadening becomes very small for such electrons. Another use of threshold photoelectron spectrometers is in the study of threshold photo-double-ionisation where the interest lies in the motion of the two low-energy outgoing photoelectrons and the strong electron–electron correlations involved. It was for these studies that the present threshold spectrometer was built and developed. During the threshold photo-double-ionisation studies the wider advantages of the threshold spectrometer became apparent. These include: high transmission (~100%), high resolution (~3 meV), high sensitivity, relatively simple mechanical construction and stable operation. These properties suggest that the spectrometer could be useful as a diagnostic tool on synchrotron VUV and soft x-ray beam lines to test the characteristics of the photon beam.

A variety of designs of threshold photoelectron analysers have been described in the literature. The basic requirement of these analysers is that low-energy photoelectrons ($\leqslant$10 meV) should be transmitted with high efficiency (~50–100%) whilst more energetic electrons are discriminated against. In photoionisation studies, designs have been based either on angular discrimination of higher energy electrons by baffles or on time-of-flight measurements. Angular discrimination was first used by Baer *et al* (1969). In their technique, called the steradiancy technique, the photoelectrons were generated in a homogeneous electrostatic extracting field. After acceleration the electrons passed through a long tube that suppressed most of the energetic electrons since these tend to have a transverse velocity component that is too large to allow them to pass through the tube. Peatman *et al* (1975) developed this device further to eliminate spurious autoionisation peaks in photoelectron spectra. Spohr *et al* (1971) described a threshold analyser based on the same principle but with the single tube replaced by a plate containing numerous closely spaced parallel channels having a large length-to-diameter ratio. Stockbauer (1979) described an apparatus consisting of a drift tube followed by a 127° cylindrical deflection analyser. In this apparatus the photoelectrons were accelerated by some voltage, typically 3 V, and the analyser was tuned to pass only those electrons that had the energy corresponding to this acceleration voltage. In this way only electrons that were produced with a small initial kinetic energy could be detected. Time-of-flight analysers for threshold photoelectron studies have been described by, for example, Tsai *et al* (1974) and Baer *et al* (1979). These devices utilised the finite time-of-flight of the electrons before they reached the detector.

Threshold electron spectrometers have also been used in electron impact measurements. Perhaps the most successful of such spectrometers have been those based on the 'penetrating field' technique described by Cvejanović and Read (1974a). Spectrometers of this type have been used, for example, for threshold ionisation studies (Cvejanović and Read 1974b) and for threshold excitation measurements (Hammond *et al* 1985). In this technique a weak electrostatic field, sometimes having a quadrupole configuration, is allowed to penetrate into the region containing the collision volume. Scattered electrons of very low energy are collected over a wide range of initial angles by this field and are directed and accelerated towards a 90° cylindrical deflection analyser. In this way electrons of low energy, typically from 0 to about 3 meV, are detected with high efficiency whilst those of higher energy are discriminated against. This penetrating field technique has been used in the present spectrometer. The main differences between the present spectrometer and the earlier penetrating field devices are the use of a 127° cylindrical deflection analyser (CDA) and the provision of an electrostatic lens to match the CDA to the penetrating field extractor stage. The purpose of the CDA is to discriminate against non-threshold electrons that leave the interaction region in the direction of the exit hole, and that would otherwise produce a tail on the high energy side of the response function of the spectrometer.

2. Constructional details

A schematic diagram of the threshold photoelectron spectrometer is shown in figure 1. The essential parts of the spectrometer are: the cage surrounding the interaction region, the extracting electrode outside the exit aperture of the cage, an asymmetric electrostatic lens, a 127° CDA and an electron detector.

The cage surrounding the interaction region is a crucial part of the spectrometer and is illustrated schematically in figure 2. The cage must allow penetration of the extracting field and passage of the photon beam and yet allow energetic photoelectrons to leave the region without producing low energy secondary electrons at solid surfaces. Such low energy secondary electrons would tend to be drawn into the threshold spectrometer and thus contribute a spurious background signal. The target cage is therefore designed and constructed to make it as transparent as possible. The framework of the cage is 40 mm high and has a diameter of 20 mm and is constructed from

† Permanent address: Department of Physics, Technical University, 80-952 Gdańsk, Poland.

0022-3735/87/040440 + 04 $02.50

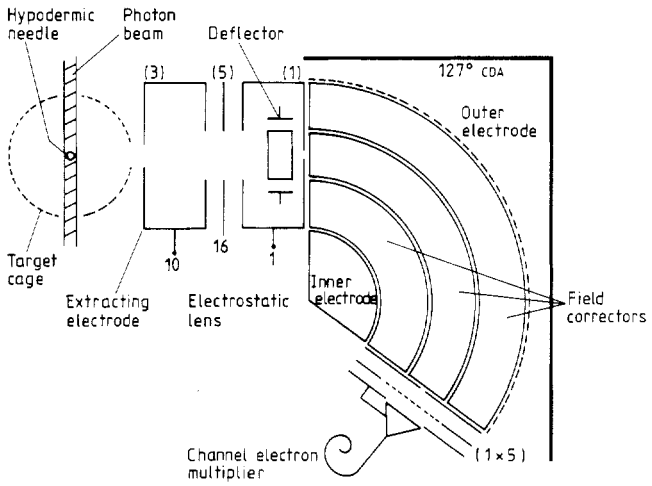

Figure 1. Schematic diagram of the spectrometer. The target gas beam enters from below (i.e. perpendicular to the plane of the paper) through the hypodermic needle while the photon beam is perpendicular to the gas beam direction and the optical axis of the extraction and lens system. The numbers below the electrodes indicate typical applied voltages measured with respect to the local earth of the spectrometer (see text). The numbers in parenthesis above the electrodes indicate diameters of apertures in mm.

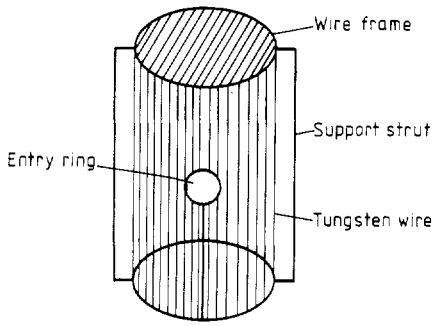

Figure 2. Schematic diagram of the cage surrounding the interaction region. Only one of the three entry or exit rings is shown.

Advance wire of diameter 0.5 mm. Upon this framework is wound 0.02 mm diameter tungsten wire spaced at 2 mm intervals. The use of thin wire rather than mesh results in a higher transparency of the target cage, a value of approximately 98% being achieved. The struts that support the upper and lower parts of the frame are situated outside the shielding wires, again minimising the probability of low energy secondary electrons being drawn into the analyser. Three rings attached to the frame provide entry and exit holes for the photon beam and entry for the extracting field. These rings have a diameter of 3 mm. After construction the whole assembly was gold plated to minimise the effects of contact potential variations.

The target gas beam emanates from a gold-plated platinum–iridium hypodermic needle of bore 0.5 mm. This hypodermic needle is positioned on the central axis of the target cage and is electrically isolated from the rest of the interaction region so that its potential can be altered to optimise the performance of the spectrometer. The potential difference between the tube and the rest of the interaction region is typically tens of mV. The orifice of the hypodermic needle is placed approximately 3 mm from the photon beam axis for optimum performance of the spectrometer.

An electrode which has an aperture of diameter 3 mm is situated 2 mm outside one of the exit holes of the cage. This electrode produces the extracting field that draws out the low energy photoelectrons and directs them towards the analyser.

The effect of the extracting field on the threshold photoelectrons is illustrated in figure 3, which shows the computed trajectories of electrons that are produced at the centre of the interaction region with an initial kinetic energy of 2 meV. As can be seen, electrons having an energy as low as this are collected over 4π sr, and form a crossover near the exit hole of the target cage.

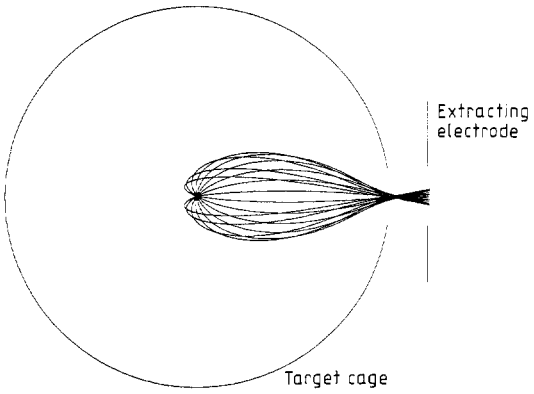

Figure 3. Computed trajectories of low energy (2 meV) photoelectrons produced at the interaction region.

The beam crossover region is imaged onto the entrance plane of the CDA by a three-aperture asymmetric-voltage lens that has a spacing (A) to bore (D) ratio of 0.5 and a value of D of 6 mm. The object and image distances are $3D$. The focal properties of the lens are given by Harting and Read (1976). The operating voltages of the lens are shown in figure 1 and are measured with respect to the local earth of the spectrometer which corresponds to the zero of electron kinetic energy. Angular definition of the electron beam is essentially provided by the extracting stage and so an additional pupil is not necessary. A single set of electrostatic deflectors is used to steer the electron beam into the CDA.

The 127° CDA has a mean radius of 25.4 mm, inner and outer electrodes of radii 12.7 and 38.2 mm respectively and a height of 45 mm. The relatively large gap between the inner and outer electrodes helps in the minimisation of the effects of patch fields and of noise due to electrons being scattered off the outer electrode. Possible problems due to fringing fields were minimised by the use of Jost correctors (Jost 1979) at the entrance and exit planes of the analyser and similar field correctors at the top and bottom of the CDA, as shown in figure 1. The central field-correcting electrodes would normally be held at the mean analysing potential of the analyser but it was found useful to superimpose small potentials (of magnitude $\leqslant 0.2$ V) on these electrodes to produce a deflecting action on the electrons and so maximise the transmitted signal. A real aperture of diameter 1 mm is placed at the entrance plane of the CDA while a slit of dimensions 1×5 mm is placed at the exit plane. The analyser can be operated at pass energies as low as 0.3 eV, giving a bandpass of 0.015 eV, over periods of several weeks with excellent stability. The inner electrode is solid while the outer electrode is made from high transparency mesh clamped in a simple frame. There is no evidence of noise arising from electrons scattered off surfaces in the CDA.

It would be possible and perhaps advantageous to use a hemispherical deflection analyser, although it would be more difficult to construct the outer hemisphere from mesh of high transparency.

A channel electron multiplier with a conical input (Mullard B419/01) is used to detect transmitted electrons and a potential of 25 V is applied to its input to optimise the electron detection

efficiency. Any possible field penetration from the channel electron multiplier into the analyser is minimised by a fine mesh screen placed between the two.

Molybdenum is used for all electrodes that are exposed to the electron beam. Other mechanical parts of the threshold spectrometer are constructed from aluminium, which is non-magnetic, is easy to machine and presents no problems due to outgassing. Since the electron energies in the spectrometer are low, it is essential to bake the whole spectrometer continuously. A temperature of 100 °C was found to be adequate. The baking is conveniently achieved by resistive heating of 0.25 mm diameter nichrome wire that is wound non-inductively in four-bore ceramic rods distributed around the spectrometer. A heating power of 35 W is used. The sum of the ripple and noise voltages on all the electron optical elements is less than 2 mV peak to peak.

The spectrometer is housed in a stainless steel vacuum chamber of diameter 350 mm which is pumped by a 510 l s^{-1} turbomolecular pump (Balzers type TPU510). A mumetal shield and a single pair of Helmholtz coils placed in a horizontal plane are used to keep magnetic fields in the interaction region less than 5×10^{-7} T.

3. Performance of the spectrometer

To test the spectrometer it was attached to a toroidal grating monochromator (TGM) on the Daresbury Laboratory Synchrotron Radiation Source. This provides radiation over the range 10–100 eV within an energy band as small as 0.015 eV. Photons from the output of the TGM were transported to the interaction region by a Pyrex capillary tube of internal bore 2 mm. The exit of the tube was placed 5 mm from the entrance ring in the cage surrounding the interaction region. Care was taken to minimise noise due to background photons. The photon flux passing through the interaction region was measured using a combination of a sodium salicylate film and a photomultiplier tube that had been previously calibrated against a standard photodiode.

In the present measurements the yield of threshold electrons is measured as the incident photon energy is varied across the region of interest. Output pulses from the electron detector are amplified, shaped and counted and their numbers are stored in a PDP11 minicomputer operating in a multiscaling mode. The minicomputer also changes the energy of the photon beam in synchronism with the channel address via a stepper motor attached to the grating of the TGM. The photomultiplier signal is used to ensure that each channel dwell time corresponds to the same number of incident photons at the interaction region.

3.1. Threshold photoionisation measurements in argon

Argon is a convenient atom with which to test the performance of the spectrometer for several reasons. Its threshold photoionisation spectrum is simple, the photoionisation cross sections have been well studied and there exist Rydberg states 11s′, 12s′, 13s′, 14s′, etc, that converge to the $^2P_{1/2}$ state of Ar^+ and which autoionise, leading to the production of electrons with energies of 3, 38, 62, 81 meV, etc respectively. The ability of the spectrometer to suppress the more energetic of these electrons is a good test of its performance. The threshold spectrum shown in figure 4 demonstrates the high performance of the spectrometer. Threshold electrons are produced as the photon energy crosses the energies of the $^2P_{3/2}$ and $^2P_{1/2}$ states of Ar^+ at 15.760 and 15.938 eV respectively. The photon energy scale was calibrated by making measurements of the photoabsorption spectrum of N_2 in the same energy region. This gave an uncertainty in the energy scale of ±3 meV. The observed positions of the peak maxima in the spectrum shown in figure 4 are 15.760 and 15.937 eV respectively, in agreement with the spectroscopic

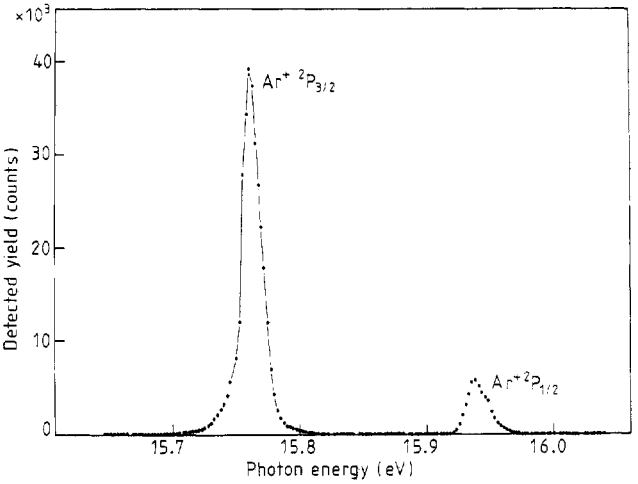

Figure 4. Threshold photoionisation spectrum of argon in the region of the $^2P_{3/2,\,1/2}$ states of Ar^+. The channel width is 2.5 meV. The observed ratio of peak heights is 6.7 : 1.

values. The fact that the maxima of the threshold peaks occur at the spectroscopic values indicates that the widths of the peaks are determined by the energy spread of the photon beam, and that the energy resolution of the threshold spectrometer is much smaller than the observed widths of the peaks. The photon flux in this measurement was approximately 2×10^8 photons/s, while the estimated target gas pressure was 2 Pa. The count rate in the $^2P_{3/2}$ peak was 4×10^4 counts/s, while the signal-to-noise ratio was approximately 10^3 : 1 as is clearly demonstrated by the almost complete absence of noise in the energy region between the two peaks.

As can be seen from figure 4 there is no evidence of a peak at the energy (15.798 eV) of the 12s′ autoionising state which gives rise to electrons of energy 38 meV. The 11s′ autoionising state lies just 3 meV above the $^2P_{3/2}$ ion state and so the ejected electrons cannot be resolved in energy from the threshold electrons by the spectrometer. The ejected electrons therefore add to the intensity of the peak corresponding to the $^2P_{3/2}$ ion state, which explains why the ratio of the heights of the two peaks is not the ratio of statistical weights, 2 : 1. The observed ratio of the peaks is 6.7 : 1 which indicates (Peatman *et al* 1975) that the energy resolution of the spectrometer is approximately 3 meV. This cannot be deduced directly from the observed width (FWHM = 17 meV) of the peaks in the threshold spectrum since this width is dominated by that of the incident photon beam.

3.2. Threshold photoionisation measurements in helium

The initial reason for constructing the spectrometer was to study photo-double-ionisation processes in helium (King *et al* 1986). Here doubly excited states close to the double ionisation potential (79.005 eV) are of interest as well as the continuum above the double ionisation potential. The photoionisation cross sections in this region are small ($\leqslant 10^{-20}$ cm^2) and so the spectrometer must have high transmission for the threshold electrons that are produced. In these measurements there is also present a large yield of much more energetic (~55 eV) photoelectrons that arise from the more probable process of excitation of the $He^+(1s)$ state. It is these energetic electrons that could strike the cage surrounding the target region and produce low energy secondary electrons that could constitute an unwanted background. A threshold spectrum covering the region of the $He^-(n=2)$ states is shown in figure 5. The photon energy scale has been calibrated by assuming that the maximum of the threshold peak occurs at the spectroscopic value of the ion state, namely 65.401 eV (Martin 1973). The photon flux in

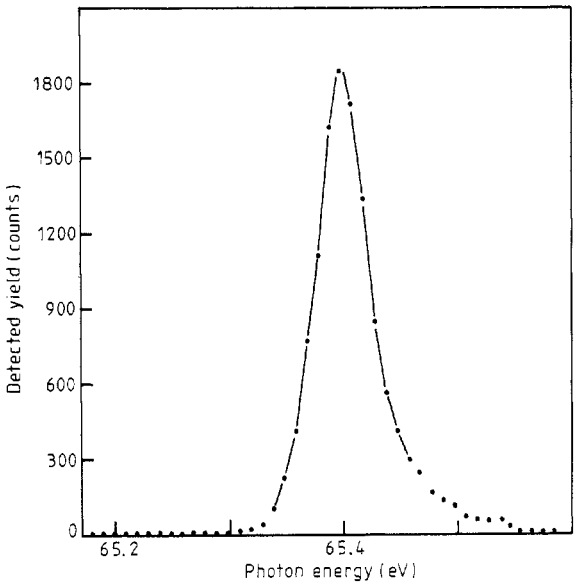

Figure 5. Threshold photoionisation spectrum of $He^+(n=2)$. The signal-to-noise ratio in the peak is 185 : 1. The channel width is 10.0 meV.

this measurement was approximately 1×10^9 photons/s and the estimated target gas pressure was 6 Pa. The count rate in the $He^+(n=2)$ peak was 505 counts/s. The width of the peak is 55 meV (FWHM) and corresponds to the energy width of the photon beam. The high signal-to-noise ratio of the spectrum, 185 : 1, demonstrates the high rejection ratio for non-threshold photoelectrons.

3.3. The use of the spectrometer for non-threshold photoelectrons

The present spectrometer has been designed primarily for the detection of threshold electrons of near-zero energy. It is however, unlike most other threshold analysers, also able to handle non-threshold photoelectrons (>10 meV). For this mode of operation the extracting electrode is electrically connected to the target region whose potential then corresponds to the primary kinetic energy of the photoelectrons. The instrument then becomes a conventional photoelectron spectrometer. The object of the electrostatic lens is the interaction region, increasing the object distance by about $1.5D$. The focal properties of the three-aperture lens can be easily adjusted to accommodate this change. The extracting electrode becomes the pupil of the system and defines the half angle of the electron beam to be 7°. Using the spectrometer in this mode of operation photoelectrons of energies from a few eV up to 55 eV were collected and energy analysed. It was also found possible to use the spectrometer to cover the more difficult energy region between threshold and 2 eV above threshold (Zubek *et al* 1986).

4. Summary

A new threshold spectrometer has been described and its performance demonstrated. It features high collection efficiency and transmission of threshold electrons, high energy resolution, high rejection of non-threshold electrons and high stability. It is primarily for use in threshold studies but it can also be used in a mode that is suitable for non-threshold photoelectron studies.

Acknowledgments

We are grateful to the SERC for financial support, for a Research Studentship for one of us (PMR) and a Research Assistantship for another of us (MZ). We gratefully acknowledge the staff at Daresbury Laboratory for help with the TGM and the computing equipment.

References

Baer T, Guyon P M, Nenner I, Tabche-Fouhaille A, Botter R, Ferreira L F A and Govers T R 1979 Non-Franck–Condon transitions in resonant autoionization of N_2O
J. Chem. Phys. **70** 1585–92

Baer T, Peatman W B and Schlag E W 1969 Photoionization resonance studies with a steradiancy analyser. II. The photoionization of CH_3I
Chem. Phys. Lett. **4** 243–7

Cvejanović S and Read F H 1974a A new technique for threshold excitation spectroscopy
J. Phys. B: At. Mol. Phys. **7** 1180–93

Cvejanović S and Read F H 1974b Studies of the threshold electron impact ionization of helium
J. Phys. B: At. Mol. Phys. **7** 1841–52

Delwiche J, Hubin-Franskin M J, Guyon P M and Nenner I 1981 Autoionization of OCS by threshold photoelectron spectroscopy
J. Chem. Phys. **74** 4219–27

Hammond P, King G C, Jureta J and Read F H 1985 The threshold electron spectrum of carbon monoxide
J. Phys. B: At. Mol. Phys. **18** 2057–73

Harting E and Read F H 1976
Electrostatic Lenses (Amsterdam: Elsevier)

Jost K 1979 Fringing field correction for 127° and 180° spectrometers
J. Phys. E: Sci. Instrum. **12** 1001–5

King G C, Zubek M, Rutter P M and Read F H 1986 A study of the threshold photoelectron spectrum of helium
J. Phys. B: At. Mol. Phys. to be published

Martin W C 1973 Energy levels of neutral helium
J. Phys. Chem. Ref. Data **2** 257–66

Peatman W B, Borne T B and Schlag E W 1969 Photoionization resonance spectra 1. Nitric oxide and benzene
Chem. Phys. Lett. **3** 492–7

Peatman W B, Gotchev B, Gurtler P, Koch E E and Saile V 1978 Transition probabilities at threshold for the photoionization of molecular nitrogen
J. Chem. Phys. **69** 2089–95

Peatman W B, Kasting G B and Wilson D 1975 The origin and elimination of spurious peaks in threshold electron photoionization spectra
J. Electron Spectrosc. Rel. Phenom. **7** 233–46

Spohr R, Guyon P M, Chupka W A and Berkowitz J 1971 Threshold photoelectron detector for use in the vacuum ultraviolet
Rev. Sci. Instrum. **42** 1872–9

Stockbauer R 1979 Threshold photoelectron spectra of atmospheric molecules, I. Description of method and application to H_2, D_2 and N_2
J. Chem. Phys. **70** 2108–14

Tsai B, Baer T and Horovitz L 1974 A time-of-flight detection system for near threshold photoelectron spectroscopy
Rev. Sci. Instrum. **45** 494–8

Zubek M, King G C, Rutter P M and Read F H 1986 Measurements of photoionisation functions of ionic states of helium and nitrogen
J. Phys. B: At. Mol. Phys. to be published